X-640-65-273

NASA TM X-55234

DIFFUSION OF PROTONS IN THE OUTER RADIATION BELT

BY

M. P. NAKADA

G. D. MEAD

JUNE 1965

GODDARD SPACE FLIGHT CENTER
GREENBELT, MARYLAND

Submitted to Journal of Geophysical Research

Diffusion of Protons

in the Outer Radiation Belt

by

M. P. Nakada

and

G. D. Mead

Goddard Space Flight Center

Greenbelt, Maryland

ABSTRACT

27825

The diffusion of protons in the outer radiation belt due to violation of the third adiabatic invariant has been examined. The particular mechanism studied is one where variations in the solar-wind intensity produce magnetic disturbances causing motion of particles between L-shells. A Fokker-Planck diffusion equation is used with terms describing Coulomb energy degradation and charge-exchange losses with the ambient atmosphere. A source near the magnetopause is assumed. The diffusion constant is numerically evaluated by an analysis of observed frequencies of sudden impulses and commencements. The equation is solved to obtain radial and energy distributions. A comparison of the results with the measured proton fluxes of Davis, Hoffman, and Williamson indicates that a diffusion process of this general nature seems to be responsible for the observed outer-belt protons. For the parameters selected, the magnetic disturbances studied may not be sufficient to produce the required diffusion rate. The effects of possible changes in parameters are discussed.

Author

Introduction

Recent observations by Davis and Williamson [1963] and Davis et al. [1964] in the L = 2 to 8 earth radii region of the outer radiation belt confirm the existence of large fluxes of 0.1 to 10 Mev protons. Except for the more energetic protons beyond L = 5, the intensities appear to be very stable over times of the order of years. An outstanding feature of these protons is the large but smooth variation in their spectra with L and equatorial pitch angle.

The recent theoretical study of the spectra of these protons by Dungey et al. [1965] strongly suggests that the source is near the edge of the magnetosphere and that some process that violates the third adiabatic invariant for trapped particles (i.e., permits motion between L-shells) plays an important role in populating the radiation belt. Parker [1960], Davis and Chang [1962], and Tverskoy [1964] have studied one such process which must surely operate according to present interpretations of geomagnetic fluctuations due to solar plasma.

This mechanism operates in the following way. Consider particles trapped near the equator, which drift around the earth on a constant magnetic field path. When the solar wind intensity is low and the geomagnetic field is relatively undisturbed, their drift paths may be represented by the solid line of Figure 1(a). If the solar wind intensity increases in times short compared to the longitudinal drift period of the particles, the particles will follow the lines of force as they are compressed during the magnetic disturbance. They will move into a smaller ring which is displaced away from the sun, as indicated by the dashed line in Figure 1(a) and the solid line in Figure 1(b). Different portions of the displaced ring will follow different constant magnetic field paths (dashed lines in Figure 1(b)) during subsequent longitudinal drift. In general, these paths will be closer to the earth on the dark side. Now if the solar wind decays to its original low value in times long compared to the longitudinal drift period, the third adiabatic invariant will remain valid for the particles during this slow expansion phase. The net effect is that any initially narrow ring of particles (dashed line of Figure 1(d)) will become broadened (between solid lines in Figure 1(d)) and diffusion in L-space will occur.

Sudden impulses and sudden commencements have rise times of a few minutes and decay times of a few hours. Typical protons seen by Davis et al. [1964] have drift times of the order of a half hour or so. (The drift time of equatorially-trapped, non-relativistic particles is 44/LE minutes [Lew, 1961], with L in earth radii and E in Mev.) Thus the protons considered here should be diffused by this mechanism.

Parker [1960] evaluated the mean square broadening per magnetic disturbance and obtained the large-L portion of the steady state distribution

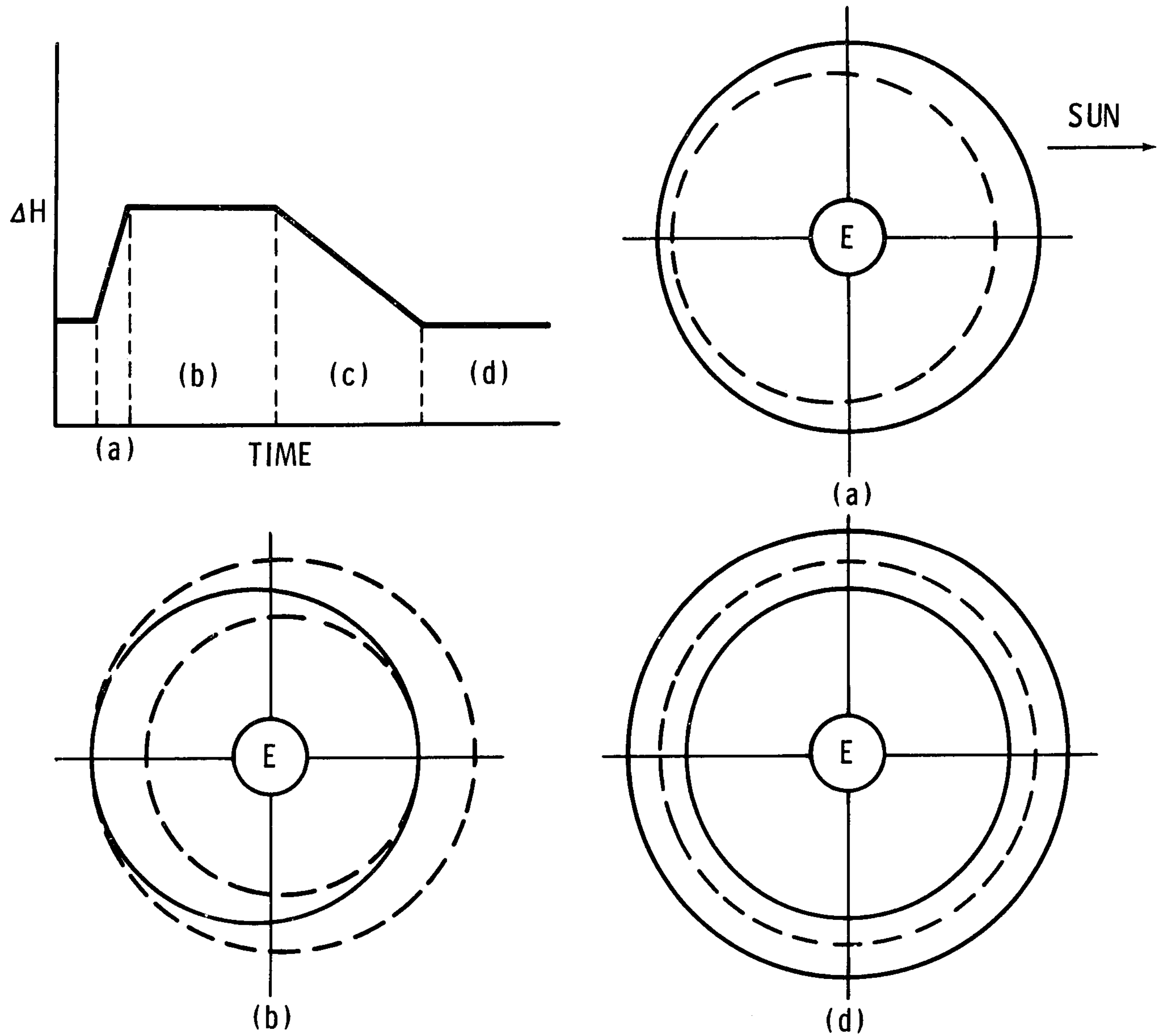

Figure 1—Schematic drawing of a sudden commencement (upper left). The behavior of a ring of particles trapped near the equator during corresponding phases of the sudden commencement is shown schematically in (a), (b), and (d). See test for details.

of electrons by using a diffusion equation and considering many disturbances. Davis and Chang [1962] found that for this mechanism the Fokker-Plank equation was appropriate (see also Parker [1963], Tverskoy [1964], and Dungey [1965]). They concluded that the mean displacement of a ring of particles, $\langle \Delta r \rangle$, had a large effect on the equatorial distribution. Davis and Chang [1962] also obtained steady-state radial distributions by assuming a source near the magnetopause and assuming that the particle density vanished at a particular value of L near the earth. This latter assumption is quite reasonable, since the diffusion rate becomes small very rapidly as the earth is approached. However, unless specific loss rates are considered, it is not possible to determine where the density vanishes and, thus, the effectiveness of the mechanism.

Tverskoy [1964] added Coulomb energy loss to the Fokker-Plank diffusion equation, obtained solutions for relativistic electrons, and concluded that this mechanism was important for these electrons. He also compared diffusion times with Coulomb energy-loss lifetimes of protons and concluded that if sources existed, Mev protons and α particles should exist in the outer belt. We also made a similar comparison [Mead and Nakada, 1964]. Although this procedure does give an indication of the effectiveness of the mechanism, it is rather unsatisfactory, since the interpretation of "diffusions times" and Coulomb energy-loss lifetimes is vague and dependent on the proton spectrum.

In the present paper, therefore, we have obtained solutions to the Fokker-Planck equation containing terms describing energy losses due to Coulomb interaction with the ambient electrons as well as charge exchanges losses with the neutral atmosphere. Both radial and energy distributions are obtained.

Instead of an image dipole model of the disturbed field, we used the more accurate magnetosphere model of Mead [1964], based on the solution to the Chapman-Ferraro problem of a perfectly-conducting plasma incident upon a three-dimensional dipole field. Also, sudden commencements and sudden impulses were interpreted in terms of the compression of the magnetosphere from an initial quiet-time configuration, caused by an increase in the solar wind intensity, rather than assuming that the solar wind was absent between magnetic disturbances, as did Parker and Davis and Chang. To obtain a numerical value for the diffusion coefficient in the Fokker-Planck equation, we used an estimate of the actual number of observed sudden impulses and commencements of various amplitudes during the period 1958 to 1961.

The solutions to the equation were then converted to integral fluxes $j(>E)$ corresponding to the seven energy thresholds of Davis and Williamson's detector. The resulting theoretical curves were compared with their experimental fluxes. The curves are remarkably similar, indicating that a diffusion process of this general nature seems to be responsible for the observed outer belt proton fluxes. Finally, the effects of modifying the various coefficients in the Fokker-Planck equation are discussed.

Steady-State Solutions

Many of the simplifying assumptions that have characterized previous calculations have been retained. The direction of the solar wind is assumed to be perpendicular to a dipole geomagnetic field. Only near-equatorial protons are considered. The magnetic moment and longitudinal invariants for the protons are assumed to remain constant during L-motion. Pitch angle changes due to the ambient atmosphere, which should be small, have been neglected. A steady source has been assumed near the quiet time magnetopause, which we assume is at 10 earth radii in the solar direction. We have also assumed that the mechanism applies out to distances quite near the magnetopause.

We consider a distribution function, $y(\mu, r, t)\, d\mu\, dr$, equal to the number of protons in dr at geocentric radius r, with magnetic moments in the interval $d\mu$ at μ, and with equatorial pitch angles (EPA) between $\pi/2 - \delta_0(r)$ and $\pi/2 + \delta_0(r)$, where $\delta_0(r)$ is a small angle whose changes with r are determined by the preservation of the magnetic moment and longitudinal invariants. This distribution function is essentially equivalent to Davis and Chang's ϕ^*. The magnetic moment $\mu = E/B = r^3 E/M$, with energy E in Mev has been used. With r in earth radii, M = 0.312 gauss. In Figure 2, μ is plotted versus E for a number of r values.

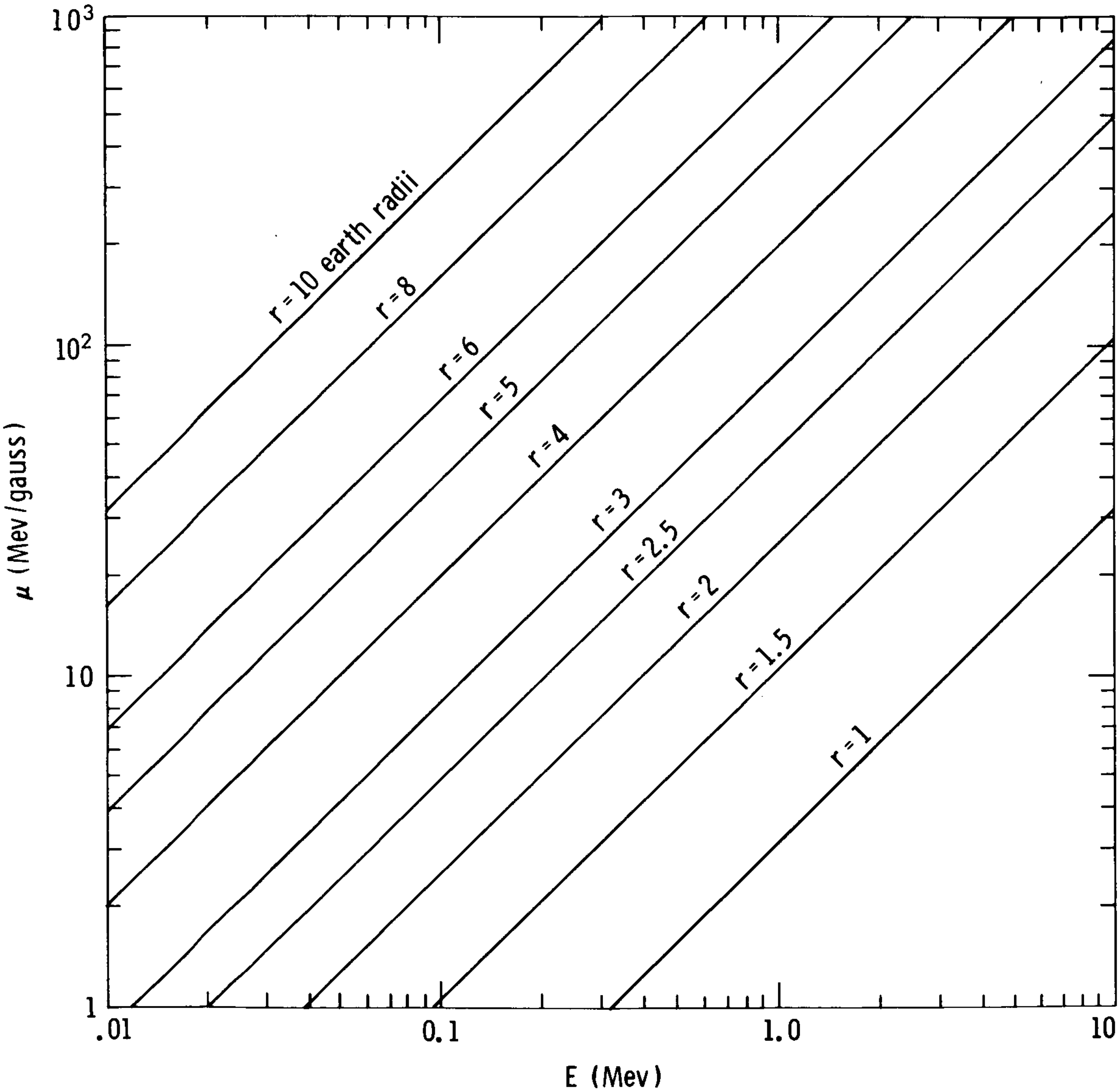

Figure 2–The relationship between the magnetic moment μ and the proton energy at various geocentric distances for particles trapped near the equator.

The magnetic moment, μ, is used in the distribution function, rather than energy, because as particles move in L-space, μ is constant except for Coulomb losses, whereas the energy varies with r.

The Fokker-Plank equation with loss terms is then [Davis and Chang, 1962; Parker, 1963]:

$$\frac{\partial y}{\partial t} = -\frac{\partial}{\partial r}\left[\left\langle\frac{\Delta r}{\Delta t}\right\rangle y\right] + \frac{1}{2}\frac{\partial^2}{\partial r^2}\left[\left\langle\frac{(\Delta r)^2}{\Delta t}\right\rangle y\right] - \frac{\partial}{\partial \mu}\left[\left\langle\frac{\Delta \mu}{\Delta t}\right\rangle y\right] - \frac{y}{\tau_{cx}} \cdot \quad (1)$$

The angular brackets denote averages over many storms and τ_{cx} is the 1/e charge-exchange lifetime. For steady-state solutions, $\partial y/\partial t = 0$.

In the evaluation of the averages in the first two terms on the righthand side of equation (1), $\langle\Delta r\rangle$ and $\langle(\Delta r)^2\rangle$ have first been evaluated for a single sudden commencement; then, time averages have been obtained by considering disturbances of all sizes and the rate of occurrence of these disturbances. For any single event, the deformation of the magnetic field by the solar wind is used to evaluate $\langle\Delta r\rangle$ and $\langle(\Delta r)^2\rangle$. Mead [1964] and Midgley [1964] have described this deformation with spherical harmonic expansions. They find that the distorted field is adequately described out to distances quite near the magnetopause by the use of two coefficients in the expansion. Higher-order terms in the more precise description of the distorted field have been found to have little effect on this mechanism.

Since the image dipole description of the distorted field as used by Parker [1960] and Davis and Chang [1962] is a special case of the two-coefficient spherical harmonic expansion, their results for $\langle \Delta r \rangle$ and $\langle (\Delta r)^2 \rangle$ have been used, with changes in only the values of the harmonic coefficients.

In prior calculations of $\langle (\Delta r)^2 \rangle$, the solar wind was assumed to be absent between world-wide magnetic disturbances. Recent measurements of both solar wind parameters [Snyder and Neugebauer, 1964] and the magnetospheric boundary [Ness et al., 1964] indicate that even during undisturbed times, a boundary is present at about 10 earth radii in the solar direction. In accordance with these findings, the quiet-time boundary, r_{bo}, is assumed to be at 10 earth radii.

In terms of the first two constants in the spherical harmonic description of the distorted field, the equatorial field is given by

$$B = \frac{M}{r^3} + \frac{a_1}{r_b^3} + \frac{a_2}{r_b^4} r \cos \phi \qquad (2)$$

with similar, but more complicated expressions for the distorted field off the equator. Here r and r_b (the distance to the boundary in the solar direction) are in earth radii, M = 0.312 gauss, and ϕ is the longitude measured from the local noon meridian. For the image dipole model used by Parker and by Davis and Chang, $a_1 = M/8$ and $a_2 = 3M/16$. In Mead's more accurate magnetosphere model, $a_1 = 0.816M = 0.2515$ gauss and $a_2 = 0.673M = 0.210$ gauss (compare equations (10-12) of Mead [1964] with equation (6) of Davis and Chang [1962]).

An analysis similar to Parker's and Davis and Chang's gives

$$\left\langle (\Delta r)^2 \right\rangle = \frac{25}{98}\left(\frac{a_2 r^5}{M}\right)^2 \left[\frac{1}{r_b^4} - \frac{1}{r_{bo}^4}\right]^2 \qquad (3)$$

which reduces to previous results if r_{bo} is very large. Since for a worldwide disturbance of average equatorial size ΔB,

$$\Delta B = a_1 \left(\frac{1}{r_b^3} - \frac{1}{r_{bo}^3}\right)$$

the mean square displacement may be written

$$\langle(\Delta r)^2\rangle = \frac{25}{98}\left(\frac{a_2}{M}\right)^2 \frac{r^{10}}{r_{bo}^8}\left[\left(1 + \frac{r_{bo}^3 \Delta B}{a_1}\right)^{4/3} - 1\right]^2 \qquad (4)$$

Because of the effect of induced currents in the earth and ionosphere, the disturbance in the horizontal component which is actually observed, $\Delta B'$, is about 50% larger than that produced by the compression of the magnetosphere, ΔB. Listed in Table 1 are a compilation through the courtesy of Dr. M. Sugiura of the average number of sudden impulses and sudden commencements per year of observed size $\Delta B'$ for the years

Table I

Observed frequencies of sudden commencements and sudden impulses of various sizes during the period 1958-1961.

$\Delta B'$ (gammas)	Number/Year	Relative Effect
> 100	0.5	.20
60 - 100	1.8	.25
40 - 60	2.3	.10
20 - 40	21	.29
5 - 20	61	.12
2	720	.04

1958 to 1961. (A sudden commencement is followed by the main phase of a magnetic storm; a sudden impulse is not.)

Using the values of Table I and setting $\Delta B = 2/3 \Delta B'$, and using Mead's coefficients for a_1 and a_2, the diffusion coefficient $\langle (\Delta r)^2/\Delta t \rangle$ has been evaluated with Equation (4) to give

$$\left\langle \frac{(\Delta r)^2}{\Delta t} \right\rangle = .031\, r_{bo}^2 \left(\frac{r}{r_{bo}} \right)^{10} \text{(earth radii)}^2/\text{day} \qquad (5)$$

Davis and Chang [1962] have derived a relationship between $\langle \Delta r \rangle$ and $\langle (\Delta r)^2 \rangle$:

$$\frac{\langle \Delta r \rangle}{\langle (\Delta r)^2 \rangle} = \frac{g}{2r} \qquad (6)$$

where g is a constant that appears to be independent of the harmonic coefficients. They find $g = 8$; when his equations are recast in similar form, Tverskoy [1964] finds $g = 6.5$. In the present calculations, a range of g has been used. Equation (6) has been used to obtain:

$$\left\langle \frac{\Delta r}{\Delta t} \right\rangle = \frac{.031}{2} g\, r_{bo} \left(\frac{r}{r_{bo}} \right)^9 \text{ earth radii/day.} \tag{7}$$

For the third term on the right in Equation (1), the Coulomb energy loss formula has been used:

$$-\frac{\partial E}{\partial t} = \frac{4\pi e^4 \rho \ln\Lambda}{m v}$$

where ρ is the electron density, $\ln\Lambda = 20$, m is the electron mass, and v is the proton velocity. Thus

$$\left\langle \frac{\Delta \mu}{\Delta t} \right\rangle = \frac{\partial \mu}{\partial E} \frac{\partial E}{\partial t} = -4\pi \ln\Lambda \frac{e^4 \rho}{m_e} \left(\frac{r^3}{M} \right)^{1.5} \sqrt{\frac{m_p}{2\mu}}$$

$$= -3.55 \times 10^{-6} \rho \sqrt{\frac{r^9}{\mu}} \frac{\text{Mev}}{\text{gauss-day}} \tag{8}$$

with r in earth radii and ρ in electrons/cm^3. For the electron density we have used

$$\rho = \left(\frac{8 \times 10^3}{r^4} + 50\right) cm^{-3}$$

For the charge-exchange term,

$$\frac{1}{\tau_{cx}} = \sigma \rho_0 v$$

where ρ_0 is the neutral hydrogen density, which we have taken to be

$$\rho_0 = \frac{7.35 \times 10^3}{r^5} \, cm^{-3}$$

with r in earth radii. For the charge-exchange cross-section, σ, values given by Bates and McCarroll [1962] were used. The choice of electron and neutral hydrogen densities is treated below in the Discussion section.

When these terms are put into equation (1) and $x \equiv r/r_{bo}$, Equation (1) becomes:

$$\frac{.031}{2}\left[\frac{\partial^2}{\partial x^2}\left(x^{10}\, y\right) - g\,\frac{\partial}{\partial x}\left(x^9\, y\right)\right] + .113\,\rho\, x^{4.5}\,\frac{\partial}{\partial \mu}\left(\frac{y}{\sqrt{\mu}}\right) - \frac{y}{\tau_{cx}} = 0 \qquad (9)$$

which is the same as Equation (30) of Davis and Chang [1962], except for the loss terms.

This equation has been solved numerically on a computer with boundary values at small x, large μ, and at $x = 1$. At small x, which corresponded to locations within the dense atmosphere of the earth, $\partial y/\partial x = 0$ has been used for all μ. This condition is equivalent to $y = 0$ close to the earth and gave results that were independent of the location of the inner boundary as long as it was well within the dense atmosphere.

At large μ, which corresponds to the higher energies at which protons have negligible charge exchange loss, the boundary conditions were obtained by solving Equation (9) without the charge exchange term. Except near the μ at which this boundary condition was applied, the solutions obtained were found to be insensitive to the boundary values that were used.

At $x = 1$, which corresponds to the magnetopause and the assumed source location, a source energy spectrum was used. Since the μ spectrum was found to be essentially independent of r except near the earth, a spectrum similar to those measured by Davis et al. [1964] near 4 earth radii was used. This spectrum is of the form $e^{-\mu/\mu_0}$. The qualitative results for different choices of μ_0 were similar; however, the quantitative results were strongly dependent on the source spectrum.

Figure 3 shows a distribution function plotted versus r for $\mu = 200$ Mev/gauss, for which the proton energy is 1 Mev at 4 earth radii. Coulomb loss is the only important loss process at this μ value. The dashed curve in Figure 3 was obtained by Davis and Chang [1962] with the same $g = 8$ but by arbitrarily setting $y = 0$ at $r = 3$. Since the diffusion parts of the differential equations are the same, the two curves are similar at large r, where diffusion should be dominant, and differ at small r where losses become important. Their loss rate is zero for $r > 3$ and is infinite at $r = 3$, so their curve drops very rapidly near $r = 3$. The loss rate used in these calculations for $\mu = 200$ is almost constant for all r values; the effect of this distributed source and sink is apparent in the flattened curve with slower decrease at small r.

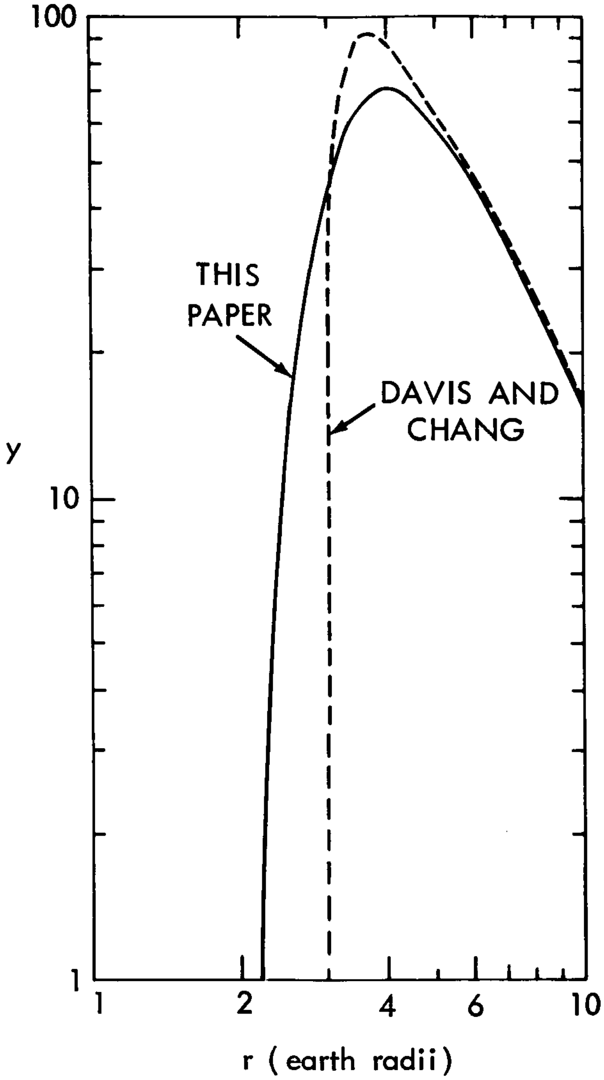

Figure 3–Comparison of the distribution functions of Davis and Chang (1962) and corresponding calculated results of this paper at $\mu = 200$ Mev/gauss, with $g = 8$. The curves have been normalized to each other at $r = 10$ earth radii. At large r, where diffusion is dominant, the curves are very similar; at smaller r, differences are due to the different treatment of loss processes.

In Figure 4, y is plotted versus r for a number of μ values. For μ greater than about 100, the curves are very similar in shape. The smaller μ curves peak at slightly larger r and drop more rapidly at small r. For $\mu = 10$, the dip at $r = 3.5$ is due to charge-exchange loss; for $r < 3.5$, there is an additional, noticeable supply of protons from larger μ values due to energy degradation.

Figure 5 shows the gradual change in the μ spectrum as protons diffuse inward. Except at small μ, the $r = 6$ curve has the same exponential form as the assumed source spectrum at $r = 10$, shown by the dashed line. At r values less than 4, the μ spectra show a gradual hardening with smaller r.

In Figures 4 and 5, y has been plotted with μ as a variable because this choice best illustrates the trends in the solutions. In the Appendix y/r is shown to be proportional to the differential flux, j (protons/cm^2-sec-ster-Mev). In Figure 6, relative differential fluxes are plotted versus r for various proton energies. In Figure 7, energy spectra are given at different r. Figures 6 and 7 do not have the same overall normalization as Figures 4 and 5.

The results shown in Figures 4 - 7 are typical in that variations in parameters such as g, the source energy spectrum, diffusion rate, and the atmosphere gave qualitatively similar results. The effects of varying the parameters are discussed in the next two sections.

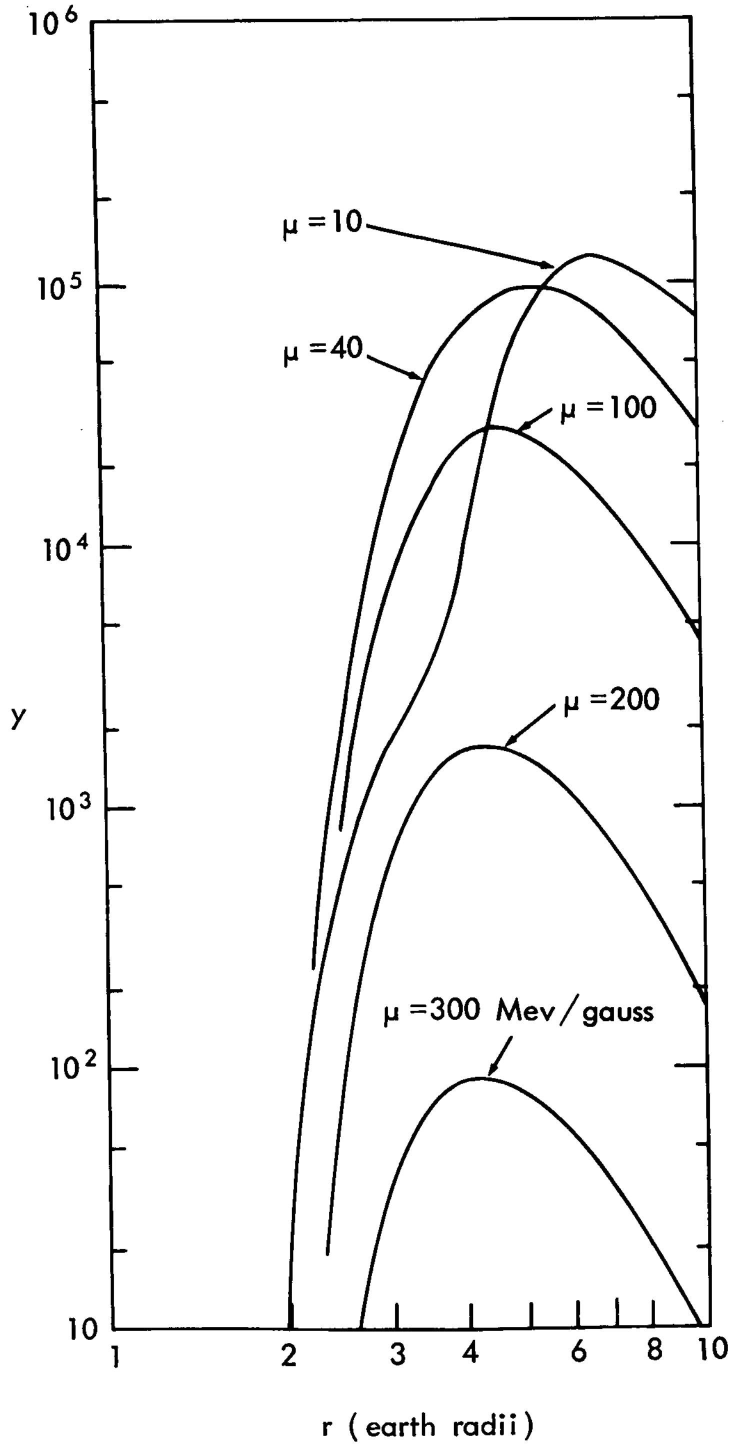

Figure 4-The distribution function at constant μ for g = 6 and μ_0 = 32 Mev/gauss.

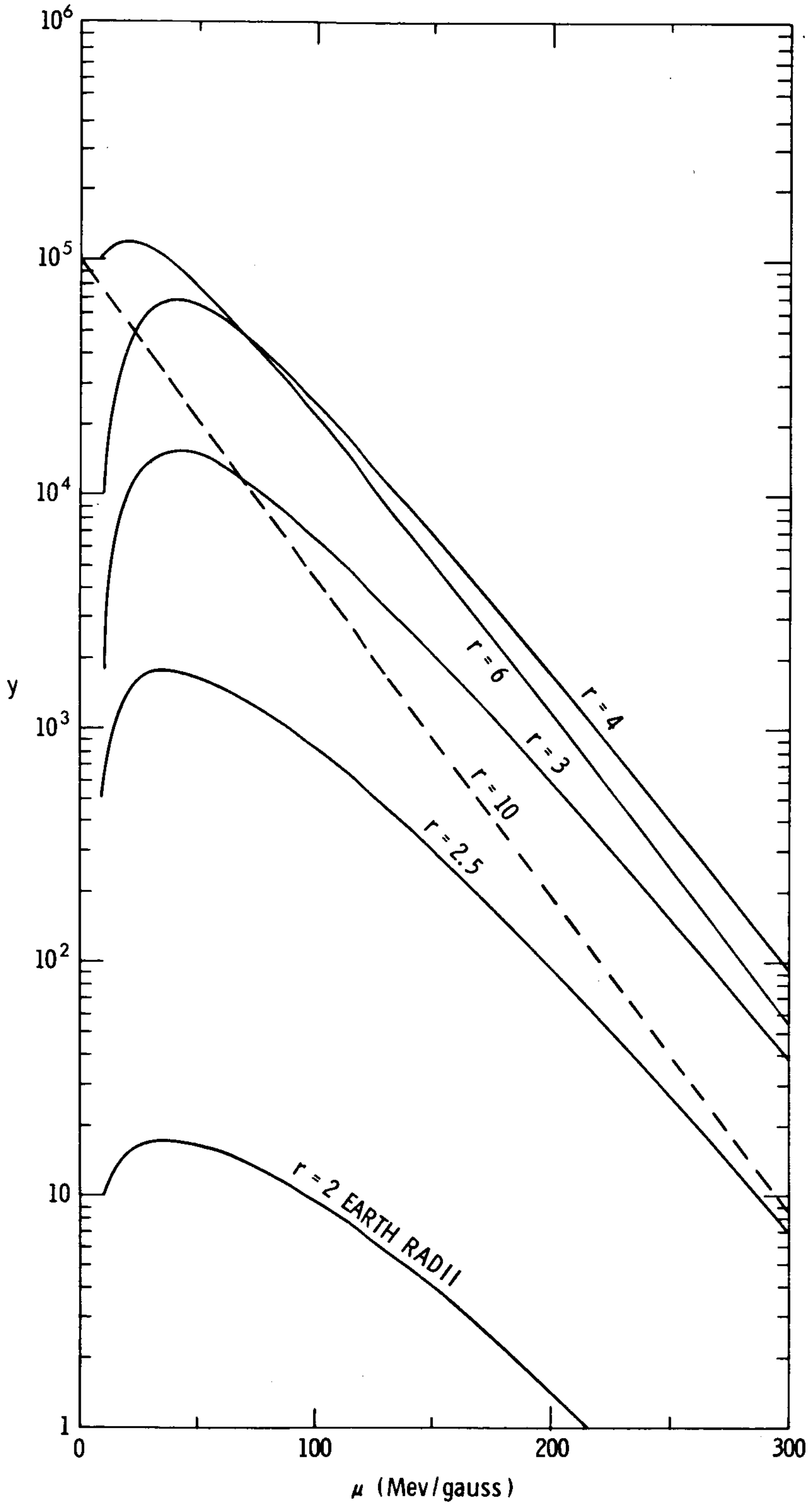

Figure 5–The μ-spectra at various geocentric distances for g = 6 and μ_0 = 32 Mev/gauss.

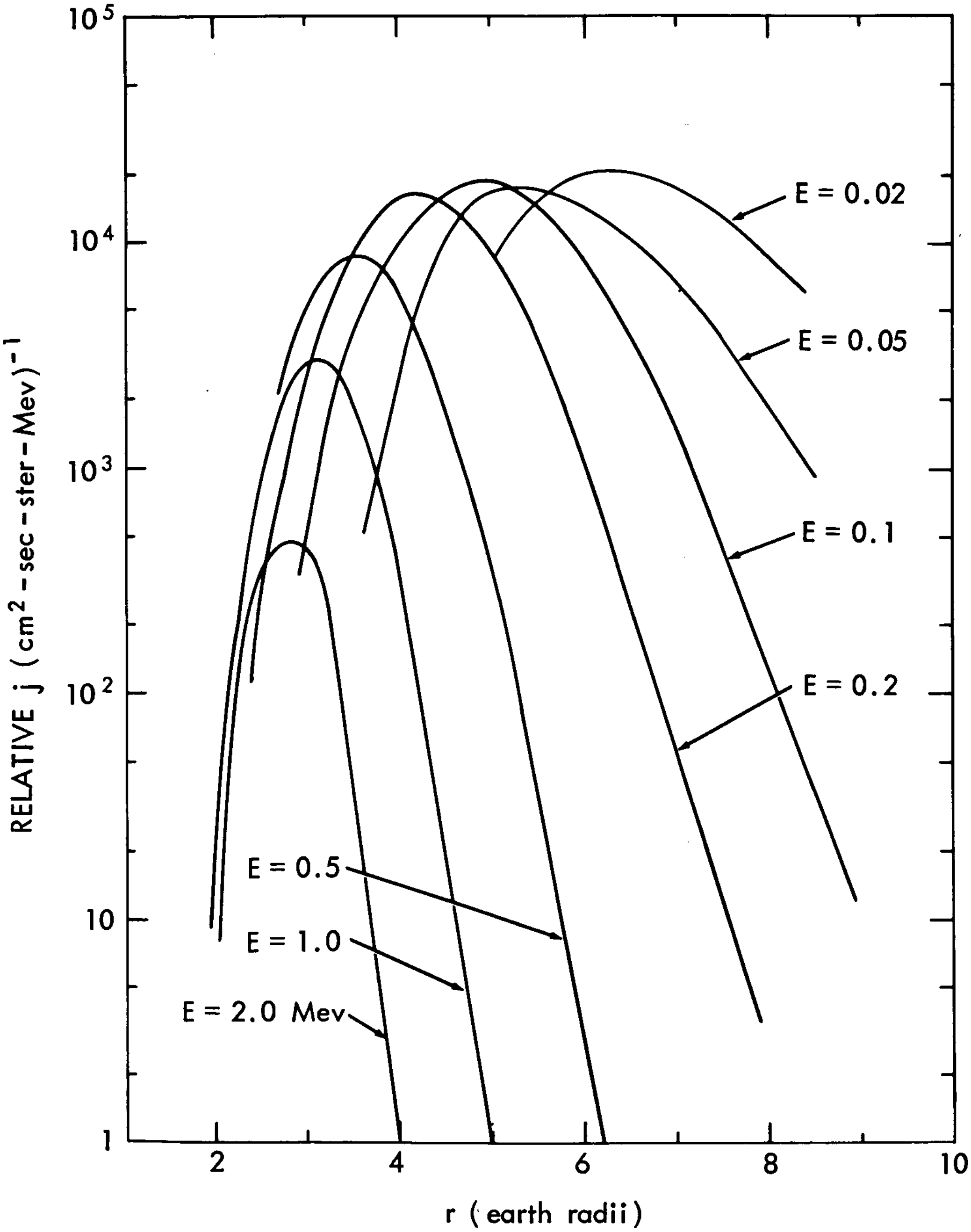

Figure 6—Relative fluxes versus geocentric distances for various proton energies. These curves are transformed from those in Figure 4.

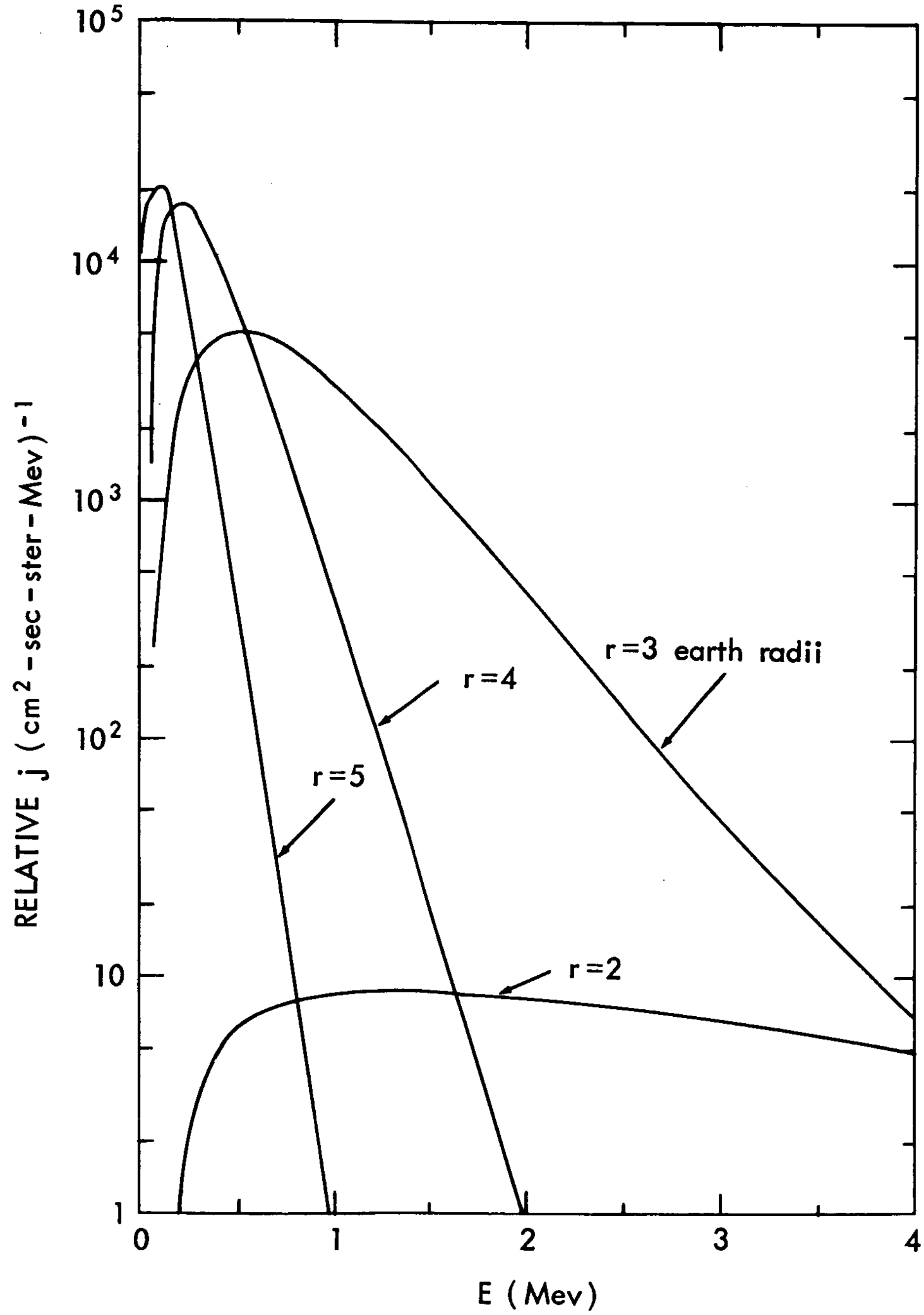

Figure 7—Energy spectra at different geocentric distances.

Comparison with Measurements

Experimental results on proton fluxes in the outer belt have been obtained with threshold detectors [Davis and Williamson, 1963] which gave fluxes, $j(>E)$, in number of protons per cm^2-sec-ster with energy greater than E. The corresponding fluxes have been calculated from our theoretical curves and are shown to the right of Figure 8. These results have been normalized to the peak flux from measurements. To the left in Figure 8 are the fluxes for near-equatorial particles that have been measured by Davis et al. [1964].

This comparison shows good qualitative similarity between the satellite measurements and the results of this model. One important quantitative difference is that the calculated curves are displaced outward by about 0.7 earth radii. This means that for the parameters that have been used, this mechanism is not effective enough to explain the measured fluxes.

Because parameters may be re-evaluated, a study has been made to see what changes in them would be required to shift the calculated curves toward lower r. In this study, the atmosphere has been kept constant, and the source spectrum has been adjusted to keep the ratio of peak fluxes for various threshold energies in agreement with

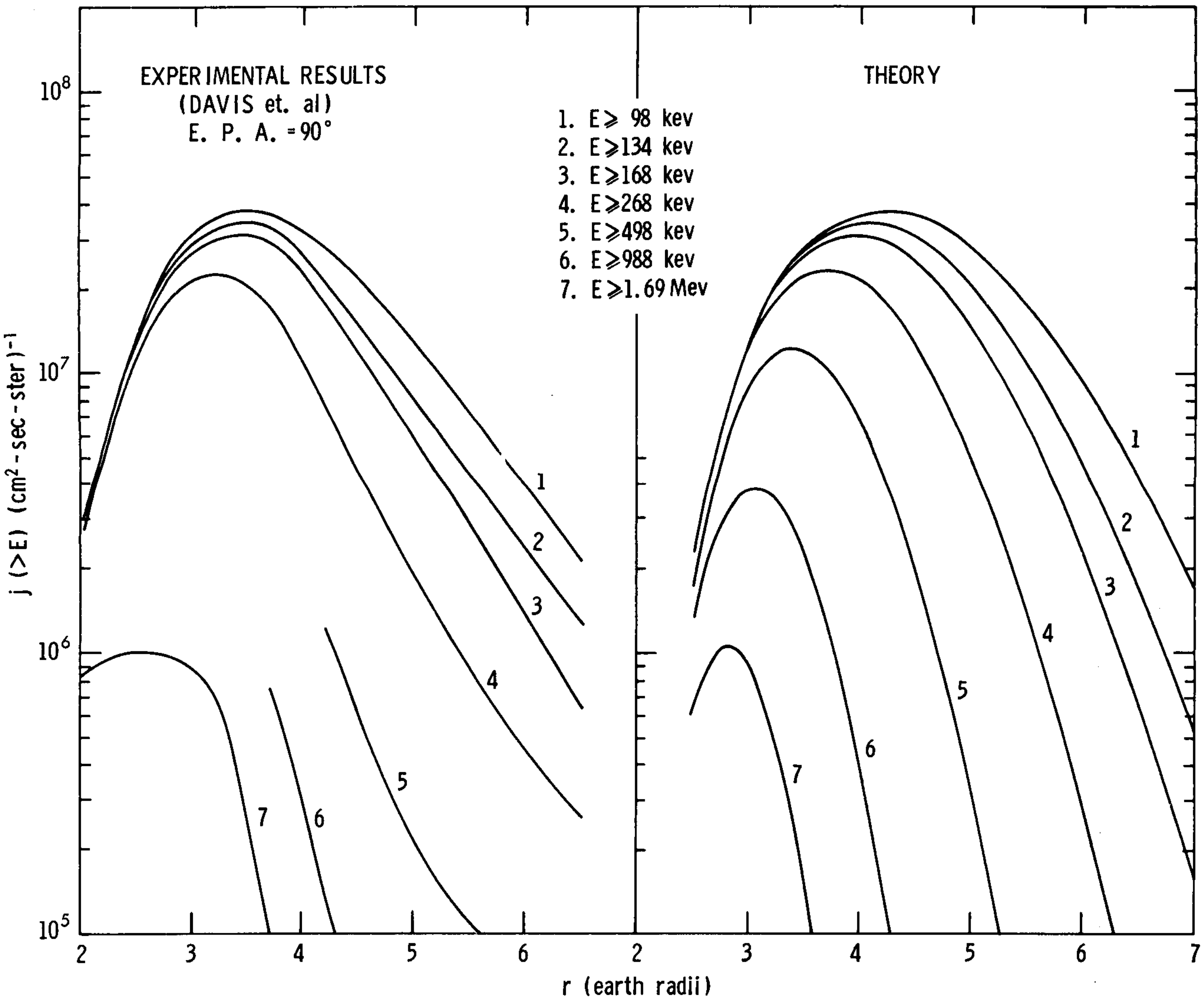

Figure 8–Comparison of integral fluxes as measured by Davis et. al. (1964) and calculated integral fluxes. The calculated curves are normalized to the same peak flux for the lowest energy threshold.

measurements. The diffusion rate, which is proportional to the constant in Equation (5) and the same constant in the first term of Equation (9), was increased for various values of g. Table II gives the factor of increase in the diffusion rate that is necessary to shift the calculated results enough to bring about agreement in r with the measured curves.

Table II

Increases in the diffusion constant in the first term of Equation (9) which are needed to give good agreement with the measured fluxes of Figure 8

g	Increase in Diffusion rate
4	x 2
5	x 3.2
6	x 5.5
8	x 8

Discussion

The results shown in Table II indicate the necessity for an increase in the diffusion rate over the value that was calculated in Equation (5) unless g is small. In this section, the various factors that entered into the evaluation of the diffusion rate are examined, and other parameters such as g and the atmosphere are discussed.

Let us assume that the numbers and magnitudes of clearly-identifiable sudden commencements and sudden impulses as given in Table I are correct. The observed magnitudes at the earth's surface are likely to be lower-limit values, since there may be attenuation of magnetic disturbances on their passage through the ionosphere. A comparison between satellite and ground measurements, such as has been made by Nishida and Cahill [1964], gives some indication of this, but more measurements are necessary. Measurements within the radiation belt of these sudden changes would be ideal for evaluating both numbers and magnitudes. Since the diffusion rate varies approximately as $(\Delta B)^{8/3}$, an attenuation of 30% would give an increase in the diffusion rate by about a factor of 2.

Table I includes only positive sudden commencements and impulses. Nishida and Cahill [1964] state that negative sudden impulses occur about half as often as positive sudden impulses. Since Parker's [1960] analysis indicates that negative impulses are as effective as positive ones in producing diffusion, the inclusion of the negative impulses would increase the diffusion rate by about 1.5 if the size distribution of negative impulses is the same as positive ones.

Table I includes only clearly-identifiable sudden impulses and commencements. But any world-wide sudden change in times of less than about 5 minutes that is followed by an unchanged field or slow decay times of about 20 minutes contributes to the diffusion rate. An examination of satellite records may be necessary to evaluate the contribution of such sudden changes that are not identifiable at the ground as sudden impulses or commencements. Some of these events are likely to produce energy and r dependent changes in the diffusion rate. The contribution of these events to the enhancement of the diffusion rate is at present unknown.

Fälthammar [1965] has developed a method for evaluating the effects of very general magnetic disturbances on the diffusion rate, whereby one makes a power spectrum analysis of the disturbance. Using this method, it would be possible to include contributions due to magnetic disturbances other than sudden commencements and impulses. Such an analysis could conceivably increase the diffusion rate substantially. Fälthammar mainly considered the possibility that time variations in electric fields would contribute to diffusion in the outer radiation belt. Unfortunately, measurements of such electric fields and their variations do not at present exist.

In the calculation of the diffusion rate, the quiet-time boundary, r_{b_o}, was assumed to be at 10 earth radii. Changes in the assumed boundary have a relatively small effect on the diffusion rate. An increase of 2 earth radii in the quiet-time boundary location reduces the diffusion rate by about 20 percent, while a decrease of 2 earth radii increases the diffusion rate by about the same amount.

The values of the two coefficients in the spherical harmonic analysis of the distorted magnetic field have a relatively large effect on the diffusion rate. As an example, if the image dipole coefficients had been used, the diffusion rate would be about eleven times more rapid than the rate for the coefficients that were used. The coefficients used give good agreement with the measurements of the shape of the magnetopause [Ness et al., 1964; Mead and Beard, 1964]. However, they are deficient in explaining the noon-midnight shift of trapped energetic electrons that are observed by polar-orbiting satellites at low altitudes and high latitudes. Willams and Mead [1965] find that good agreement with measurements can be obtained if, in addition to the magnetopause current system, a current sheet which produces a magnetospheric tail field is added. In the closed trapping region of the magnetopause, the effect of this current sheet is roughly equivalent to increasing the second harmonic coefficient. About a factor of two increase over values used here are necessary to give field distortions that are in agreement with the trapped electron asymmetry. If the current system that produces the magnetospheric tail also responds to sudden changes in the solar wind, then a factor of 2 increase in a_2 would give a factor of 4 increase in the diffusion rate, since a_2 appears squared in Equation (4). There is evidence for increases in the tail field during periods of magnetic activity [Ness, private communication]. This response of the tail field to the solar wind appears plausible, since the tail field is confined by the solar wind, and pressures within the tail depend upon solar wind parameters.

The parameter g is likely to be near the value of 6.5 or 8 that Tverskoy [1964] and Davis and Chang [1962] obtained. However, a range of g values have been used in these calculations since: (1) in determining g, they only considered a transition from no solar wind to a strong solar wind instead of from a finite solar wind to a stronger solar wind; (2) they did not consider negative sudden events or the possible coupling of these negative events with positive events; and (3) the results of the two studies are different. The g parameter was found to have a large effect on the μ distributions as in Figure 3 and 4, but a much smaller effect on the shape of integral flux curves like those in Figure 8. Thus, it does not appear possible to determine g from a comparison of calculations with experiment.

As is to be expected, both the electron and neutral hydrogen densities have a large effect on calculated results. If the densities are appreciably larger then those assumed here, then even larger increases in the diffusion rate will be necessary if the mechanism under consideration is to contribute appreciably to the explanation of the outer belt protons.

For Coulomb energy loss, only the electron density above 1.5 earth radii was found to be important. The profile that was used was obtained by using an average density at 1000 km altitude as obtained by Alouette [Thomas and Sader, 1964; Bauer and Blumle, 1964] of $6000/cm^3$, and an average density of $500/cm^3$ at 2 earth radii that is due to Bowles [1963]. An average ion mass of 6 at 1000 km was assumed with a decrease to 1 at 2 earth radii; a temperature profile due to Serbu [1965] was also assumed. A shift in the density profile to larger or smaller altitudes gave a corresponding shift in the calculated curves of Figure 8.

The neutral hydrogen density has its only appreciable effect on the lower energy protons, for which the charge-exchange cross-section is large. The four lowest-energy-threshold curves of Figure 8 were appreciably altered by changes in the high-altitude density profile. Changes in the density profile below about 4 earth radii, however, had little effect on the results. The profile that was used corresponds to the 1000°K one due to Thomas [1963] with an exospheric base density of $10^4/cm^3$ at 520 km altitude. This density was reduced by a factor of 2 beyond r = 2, in accordance with recent calculations by Liwshitz and Singer [1965].

Source Requirements

Because source requirements may help determine whether this mechanism plays an important role in populating the radiation belts, they have been estimated. These estimates have been made with the assumption that the diffusion rate is rapid enough to give agreement in the radial position of the peak fluxes between calculated and experimental results. The variation of estimated source requirements with changes in the diffusion rate and with g, however, were relatively small.

Near the subsolar magnetopause, an energy spectrum for the source of the form e^{-E/E_0}, with E_0 in the 7 to 10 kev range, gives fairly good agreement with experiment. A 2 to 3 percent addition of an exponential spectrum with E_0 near 90 kev improves the agreement of the calculated 1.688 Mev threshold fluxes with experiment. A power law spectrum of the form E^{-a}, with a near 5, also gives relative fluxes that are in good agreement with experiment.

The source strength requirement was estimated by calculating proton loss rates due to charge exchange and energy loss. First the relative total number of protons in dr at each r was calculated by evaluating $\int y \, d\mu$ over all μ. The results are shown in the top curve of Figure 9. Then the relative charge-exchange loss rate per day at each

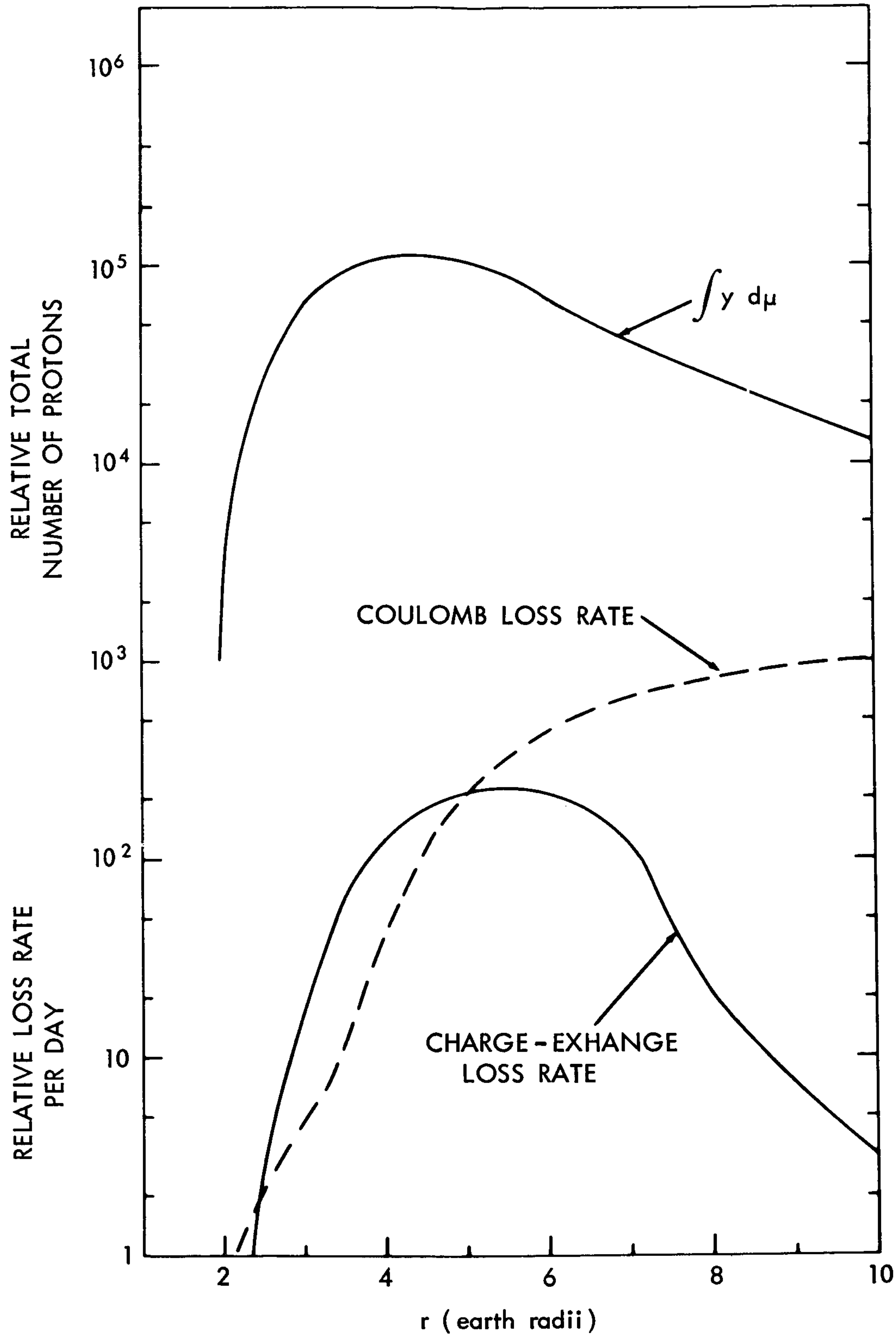

Figure 9 – Loss rates of protons in the outer belt. The top curve $\int y\,(\mu,\ r,\ t)\,d\mu$, gives the relative total number of protons in dr as a function of r. The lower solid curve, $\int (y/\tau_{cx})\,d\mu$, gives the charge-exchange loss rate per day. The lower dashed curve, $\langle \Delta\mu/\Delta t \rangle\, y$ evaluated at small μ, gives the Coulomb loss rate per day.

r was evaluated by calculating $\int \left(y/\tau_{cx} \right) d\mu$. The lower solid line of Figure 9 shows these results.

In general, Coulomb energy loss acts as a source for lower μ values. But for very small μ the degradation of energy is so rapid that the distribution function goes to zero rapidly. The product $-\langle \Delta\mu/\Delta t \rangle y$, however, remains essentially constant at small μ, and is equal to the Coulomb loss rate per day at each r. This product was evaluated at small μ, and was found to be relatively insensitive to the μ value chosen. The results are shown as a dashed line in Figure 9.

From these curves, it is evident that most of the loss occurs due to Coulomb energy degradation at large r. By comparing the integral over r of the relative loss rates with the integral over r of the total relative number of protons, we get the result that 1.2 percent of the trapped protons are lost per day. The corresponding loss rate for $r < 6$ only is about an order of magnitude less.

Assuming that the solar wind is the source of these protons, the fraction of solar wind protons which must be supplied to equal this loss rate has been estimated. The protons were assumed to fill a torus with an internal radius of 4 earth radii and a radius of 6 earth radii between the center of the earth and the locus of the internal radius. Proton fluxes were estimated from experimental results for small pitch angles. The solar wind injection area was assumed to be a circle with a radius of 4 earth radii, and a solar wind flux of 10^8 protons/cm^2-sec was also assumed. With these numbers, it was found that on the average approximately 10^{-6} of the solar wind protons must be supplied to the magnetosphere in order to replace those lost due to charge exchange and energy loss.

Whether or not sufficient protons of the required energies exist in the solar wind has not been determined. If the measured temperatures of about 10 ev and directed energies of about 1 kev in the interplanetary region are assumed, then unaltered solar wind protons do not have the necessary energies and spectrum to supply source requirements. It may be that the necessary changes occur in the transition region between the shock front and the magnetopause.

If more energetic protons from the sun or interplanetary space are the source particles, time average fluxes exceeding 10^2/cm^2-sec are required.

Conclusions

These studies strengthen the suggestion by Dungey et al. [1965] and Tverskoy [1964] that the source of the outer belt protons is near the magnetopause and that some process that violates the third adiabatic invariant is important in moving protons into the region of the outer radiation belt. Although uniqueness cannot be claimed, the similarity of the calculated fluxes to measurements gives support to the idea that some diffusion process is important.

Conclusions on whether or not this diffusion is caused exclusively or in major part by magnetic disturbances due to solar wind fluctuations must await further experimental and theoretical results. Similar conclusions may be drawn about the source and injection mechanism.

Frank et al. [1964], Frank and Van Allen [1964] and Frank [1965] have reached similar conclusions on the importance of some diffusion process in their studies of energetic electrons ($E > 1.6$ Mev) in the outer radiation belt. They further find that large variations in the source of electrons are likely. In contrast, the source for protons is likely to exhibit considerably smaller time variations, since proton fluxes at $r < 5$ earth radii are quite stable.

Although proton fluxes have been quite stable over the last few years, changes are likely to occur during other phases of the solar cycle if the processes considered here are important. Changes in parameters such as source strength, source spectrum, magnetic activity, neutral hydrogen density, and the electron density can cause predictable changes in proton fluxes and spectra. It should be interesting to follow changes in measurable parameters and proton fluxes as solar maximum is approached.

Appendix

In this appendix, the relationship between the distribution function $y(\mu, r)\, d\mu\, dr$ and the directional flux, $j(E, r, \alpha)\, dE\, dA\, d\Omega\, dt$ is derived. Davis and Chang [1962] have obtained a similar expression but with slightly different assumptions about the nature of the fluxes. Here j at the equator is assumed constant at any r over the pitch angle range from $\pi/2 - \delta_0$ to $\pi/2 + \delta_0$ where δ_0 is a small angle whose change with r is determined by the preservation of the magnetic moment and the longitudinal invariant. Only those particles with equatorial pitch angles between $\pi/2 - \delta_0$ and $\pi/2 + \delta_0$ contribute to y.

Thus y is given by:

$$y = 2\pi r \int_{-\lambda_m}^{+\lambda_m} \int_{\pi/2-\delta}^{\pi/2+\delta} \frac{j}{v} \frac{dE}{d\mu}\, 2\pi \sin\theta\, d\theta\, r\, d\lambda \qquad (1A)$$

where θ is the pitch angle, $\delta(\lambda, r)$ varies with λ the latitude, since pitch angles change with λ, and $\pm\lambda_m$ corresponds to the mirror latitude for a proton with equatorial pitch angle, $\pi/2 \pm \delta_0$.

The integration over θ gives the result:

$$y = (2\pi r)^2 \frac{j}{v}\frac{dE}{d\mu}\int_{-\lambda_m}^{\lambda_m} 2\sin\delta\, d\lambda \tag{2A}$$

From the magnetic moment invariant, the following are obtained:

$$\sin^2\left(\frac{\pi}{2} - \delta\right) = \frac{B}{B_0}\sin^2\left(\frac{\pi}{2} - \delta_0\right)$$

$$\sin^2\left(\frac{\pi}{2} - \delta_0\right) = \frac{B_0}{B_m} = \frac{\sqrt{1 + 3\sin^2\lambda_m}}{\cos^6\lambda_m}$$

$$= 1 - \frac{9}{2}\lambda_m^2$$

for λ_m small. Also

$$\sin\delta = \frac{3}{\sqrt{2}}\left(\lambda_m^2 - \lambda^2\right)^{1/2}$$

for λ and λ_m small.

Using these results, Equation (2A) becomes:

$$y = C r^2 \frac{j}{v} \frac{d\mu}{dE} \lambda_m^2 \qquad (3A)$$

where C is a constant.

When λ_m is small, the longitudinal invariant J is:

$$J = 4 \int_0^{\lambda_m} v \cos\left(\frac{\pi}{2} - \delta\right) r \, d\lambda$$

$$= K v r \lambda_m^2$$

where K is a constant.

Using this result, the result that $dE/d\mu$ is proportional to r^3, and that v^2 is proportional to $1/r^3$, Equation (3A) is:

$$y \alpha r j$$

Acknowledgments

We gratefully acknowledge the many discussions with Mr. Leo Davis and the use of his data prior to publication. Dr. M. Sugiura kindly compiled the data on sudden commencements and impulses for us. We also acknowledge the guidance of Mr. William Cahill, Dr. Arnold Stokes, and Mr. Robert Baxter in the solution of the partial differential equation.

References

Bates, D. R., and R. McCarroll, Charge transfer, Advan. Phys. 11, 39-81, 1962.

Bauer, S. J., and L. J. Blumle, Mean diurnal variation of the topside ionosphere at mid-latitudes, J. Geophys. Res. 69, 3613-3618, 1964.

Bowles, K. L., Measuring plasma density of the magnetosphere, Science 139, 389-391, 1963.

Davis, Leverett, Jr., and D. C. Chang, On the effect of geomagnetic fluctuations on trapped particles, J. Geophys. Res. 67, 2169-2179, 1962.

Davis, Leo R., R. A. Hoffman, and J. M. Williamson, Observations of protons trapped above 2 earth radii (abstract), Trans. Am. Geophys. Union 45, 84, 1964.

Davis, Leo R., and J. M. Williamson, Low-energy trapped protons, Space Research III, 365-375, 1963.

Dungey, J. W., Effects of the electromagnetic perturbations on particles trapped in the radiation belts, Space Science Rev. 4, 199-222, 1965.

Dungey, J. W., W. N. Hess, and M. P. Nakada, Theoretical studies of protons in the outer radiation belt, Space Research V, 399-403, 1965.

Fälthammar, Carl-Gunne, Effects of time-dependent electric fields on geomagnetically trapped radiation, J. Geophys. Res. 70, 2503-2516, 1965.

Frank, L. A., Inward radial diffusion of electrons E > 1.6 Mev in the outer radiation zone, Un. Iowa Rept. 65-13, 1965.

Frank, L. A., and J. A. Van Allen, Measurements of energetic electrons in the vicinity of the sunward magnetospheric boundary with Explorer 14, J. Geophys. Res. 69, 4923-4932, 1964.

Frank, L. A., J. A. Van Allen, and H. K. Hills, A study of charged particles in the earth's outer radiation zone with Explorer 14, J. Geophys. Res. 69, 2171-2191, 1964.

Lew, John S., Drift rate in a dipole field, J. Geophys. Res. 66, 2681-2685, 1961.

Liwshitz, Mordehai, and S. F. Singer, Thermal escape and the distribution of neutral hydrogen in the earth's thermosphere (abstract), Trans. Am. Geophys. Union 46, 143, 1965.

Mead, G. D., Deformation of the geomagnetic field by the solar wind, J. Geophys. Res. 69, 1181-1195, 1964.

Mead, G. D., and D. B. Beard, Shape of the geomagnetic field solar wind boundary, J. Geophys. Res. 69, 1169-1179, 1964.

Mead, G. D., and M. P. Nakada, The Parker mechanism and protons in the outer radiation belt (abstract), Trans. Am. Geophys. Union 45, 85, 1964.

Midgley, James E., Perturbation of the geomagnetic field — a spherical harmonic expansion, J. Geophys. Res. 69, 1197-1200, 1964.

Ness, N. F., C. S. Scearce, and J. B. Seek, Initial results of the Imp 1 magnetic field experiment, J. Geophys. Res. 69, 3531-3569, 1964.

Nishida, Atsuhiro, and L. J. Cahill, Jr., Sudden impulses in the magnetosphere observed by Explorer 12, J. Geophys. Res. 69, 2243-2255, 1964.

Parker, E. N., Geomagnetic fluctuations and the form of the outer zone of the Van Allen radiation belt, J. Geophys. Res. 65, 3117-3130, 1960.

Parker, E. N., Interplanetary Dynamical Processes, Appendix B, pp. 268-270, Interscience Publishers, New York, 1963.

Serbu, G. P., Results from the IMP-I retarding potential analyzer, Space Research V, 564-574, 1965.

Snyder, C. W., and Marcia Neugebauer, Interplanetary solar-wind measurements by Mariner II, Space Research IV, 89-113, 1964.

Thomas, G. E., Lyman α Scattering in the earth's hydrogen geocorona, 1, J. Geophys. Res. 68, 2639-2660, 1963.

Thomas, J. O., and A. Y. Sader, Electron density at the Alouette orbit, J. Geophys. Res. 69, 4561-4581, 1964.

Tverskoy, B. A., Dynamics of the radiation belts of the earth, II, Geomagnetism and Aeronomy 3, 351-366, 1964.

Williams, D. J., and G. D. Mead, A nightside magnetosphere configuration as obtained from trapped electrons at 1100 km, J. Geophys. Res. 70(13), July 1, 1965.